Fermi National Accelerator Laboratory

FERMILAB-Pub-91/17-A
July 1991

Perturbations from cosmic strings in cold dark matter

Andreas Albrecht and Albert Stebbins
NASA/Fermilab Astrophysics Center
P.O.B. 500
Batavia, IL 60510

July 5, 1991

Abstract

We present a systematic linear analysis of the perturbations induced by cosmic strings in cold dark matter. We calculate the power spectrum and find that the strings produce a great deal of power on small scales. We show that the perturbations on interesting scales are the result of many uncorrelated string motions, which indicates a much more "gaussian" distribution than was previously supposed.

Cosmic strings are widely considered to be possible seeds for galaxies and larger scale structure (see, for example, these pioneering papers [1,2, 3,4,5,6,7,8,9] and the numerous papers which have followed). The idea is that a network of strings formed as defects in a symmetry breaking phase transition in the early universe. Such a network is expected to rapidly approach a "scaling solution" in which most of the properties of the network are independent of the initial details. As the network evolves, the strings attract other matter gravitationally. In this way perturbations are seeded which can grow, via gravitational collapse, into galaxies and larger scale structure.

Veeraraghavan and Stebbins [10] have developed a formalism with which to study linear perturbations induced in the surrounding matter by sources

such as strings. We have applied this formalism to a numerical realization of a cosmic string network for the case of a flat universe with cold dark matter (CDM). We describe the results in terms of a simple model which can be easily extrapolated beyond the dynamical limitations of the numerical work, and adapted to different pictures of the string network. A complete discussion of this work will appear in [11]. This letter reports the main results, which differ in major ways from earlier results based on more heuristic approaches.

The degree to which string networks have been shown to exhibit scaling behavior on cosmic timescales is still controversial [12]. For this work, however, we will assume that a realistic string network is well represented by the "scaling solution". The scaling solution provides a very convenient way to think about a cosmic string network. At any given time the strings can be divided up into long strings and loops. Most of the properties of the long strings can be described in terms of a single scale ξ defined by

$$\rho_L = \frac{\mu}{\xi^2}, \tag{1}$$

where ρ_L is the energy density in long string and μ is the mass per unit length of the string. (Except where stated otherwise, we use geometrical units, where $c = G = 1$.) The long strings describe random walks of step size ξ, and also have a mean separation of $O(\xi)$. The strings move around at relativistic speeds, but the general properties of the network at two different times are related by simply rescaling ξ appropriately. The degree to which the long string is straight on scales smaller than ξ is a subject of current debate. One possibility is that small scale structure contributes to a renormalization of μ, but does not affect the gross scaling properties. In this case one can use the renormalized μ in Eq 1 so that ξ reflects the large-scale spatial properties of the network.

The time evolution of the string network is a process of equilibration, whereby the long strings are continually chopped up into the statistically favored loops (whose size is typically smaller than ξ). As a result ρ_L decreases, and ξ grows. The expansion of the universe is described by the growth of the scale factor, $a(t)$. We consider the standard flat Friedmann-Robertson-Walker universe which has an intial radiation dominated equation of state ($\Rightarrow a(t) \propto t^{1/2}$) and which eventually becomes matter dominated ($\Rightarrow a(t) \propto t^{2/3}$). We consider strings which are produced early in the

radiation era. The canonical scaling picture dictates that, well into the radiation or matter eras, any initial conditions approach the scaling solution with $\xi \propto R_H$ ($R_H \equiv a/\dot{a}$), but not necessarily with the same constant of proportionality. During the radiation-matter transition ξ/R_H interpolates smoothly between these two constant values.

The quantity relevant to the perturbation theory is $\delta(x) \equiv (\rho_d(x) - \bar{\rho}_d)/\bar{\rho}_d$, where $\rho_d(x)$ is the density of the dark matter today, and the overbar represents the spatial average. The (linear) perturbation induced in the dark matter may be written as the convolution of the string "source" density with a suitable Green function, integrated over all time. The source density is written in terms of the string stress-energy density: $\Theta_+(x) \equiv \Theta_{00}(x) + \Theta_{ii}(x)$. In Fourier space

$$\delta_{\vec{k}} = \delta^I_{\vec{k}} + 4\pi(1+z_{eq}) \int_{\eta_i}^{\infty} T(\vec{k};\eta')\tilde{\Theta}_+(\vec{k},\eta')d\eta' \qquad (2)$$

where T is $\tilde{T}^c_2$ from [10]. The effect of perturbations other than those due to string motions on the dark matter today is represented by $\delta^I_{\vec{k}}$. This term is responsible for "compensation", in which string perturbations are canceled by other perturbations on sufficiently large scales, resulting in no net perturbation on scales too large to be affected by causal dynamics. The issue of compensation is a crucial one in these calculations and it is discussed in [11]. There we conclude that the important effects of $\delta^I_{\vec{k}}$, will be well approximated if the substitution $T \rightarrow (1+\frac{k_c}{k})^{-2}T$ is made and $\delta^I_{\vec{k}}$ is dropped explicitly from Eq 2. The scale on which compensation sets in is given by k_c.

Thus modified, Eq 2 can be squared and averaged over directions in order to study $P(k)$,the power spectrum:

$$(2\pi)^3 P(k)\delta^{(3)}(\vec{k}-\vec{k}') = 16\pi^2(1+z_{eq})^2 \int_{\eta_i}^{\infty}\int_{\eta_i}^{\infty} T(k;\eta_1)T(k';\eta_2)\left\langle \tilde{\Theta}_+(k,\eta_1)\tilde{\Theta}_+(k',\eta_2)\right\rangle d\eta_1 d\eta_2. \qquad (3)$$

The picture can be simplified by noting that although there are two integrals over conformal time, η, the only significant contributions come from times when η_1 and η_2 are reasonably close. That is because the strings configurations are uncorrelated when separated by a sufficiently long time. For large enough values of $\eta_1 - \eta_2$, $\langle\tilde{\Theta}_+(k,\eta_1)\tilde{\Theta}_+(k,\eta_2)\rangle$ will be negligibly small. As long as the correlation time of the strings is small compared with

the time over which $T(k;\eta)$ varies, we can model $P(k)$ by

$$P(k) = 16\pi^2\mu^2(1+z_{eq})^2 \int_{\eta_i}^{\infty} |T(k;\eta')|^2 \mathcal{F}(k;\eta')d\eta' \tag{4}$$

where

$$(2\pi)^3\mathcal{F}(k;\eta')\delta(k-k') \approx \int_{-\infty}^{+\infty} \left\langle \tilde{\Theta}_+(\vec{k},\eta')\tilde{\Theta}_+(\vec{k}',\eta'')\right\rangle d\eta''. \tag{5}$$

The "structure function", $\mathcal{F}(k;\eta)$, represents the power spectrum of the coherent string motions. In order to represent a scaling string network, we write $\mathcal{F}(k;\eta) = F(\xi k)$. (For some of our calculations T does vary by factors $O(1)$ over the string correlation time, but we do not expect this to introduce major errors, other than factors of $O(1)$ in the normalization.)

One of our important results is that the contributions to the power spectrum come from string motions at many different times (as one integrates Eq 4). A correct calculation of the full spectrum requires knowledge of the string network far beyond the dynamic range of any string simulation. This is where scaling is a big help. In order to calculate the power spectrum, all we really need from the simulations is the correct form for $F(\xi k)$. This only requires an understanding of the network over one coherence time (but one still must resolve a range of spatial scales).

We have chosen a general form for $F(\xi k)$ which is motivated by cosmic string physics [13]:

$$F(\xi k) = \mu^2 \frac{16}{3}\left(\frac{1}{1+\frac{2}{3}(\xi k)^2}\right). \tag{6}$$

We show in [11] that the model fits the Albrecht and Turok (AT) string network very well. Since the large scale fluctuations in the string density are just the result of uncorrelated fluctuations on the scale ξ, the structure function takes on a constant (or "white noise") form for $\lambda \gg \xi$ (where $\lambda \equiv 2\pi/k$). The coherent motions of the long strings on scales $O(\xi)$ and smaller trace out sheet-like wakes, and these result in a part of $F(\xi k)$ which goes as k^{-2}, which is characteristic of two dimensional surfaces. The structure function can be further modified to include the effects of loops, but we find in [11] that the resulting effects are negligible on the scales of interest.

For our calculations, the nature of the cosmic strings is completely specified once one fixes the compensation scale k_c and the function $\xi(\eta)$. We consider three different choices for these quantities. The "AT" parameters are $k_c = 4\pi/\eta$ and $\xi(\eta)$ given by Eq 3.7 in [14]. The "ATO" (AT old) parameters are $k_c = 4\pi/\eta$ and $\xi(\eta) = R_H/\sqrt{10}$. The ATO parameters represent the old picture of cosmic strings (as extrapolated from [15] in the simplest way), and we use them to illustrate how little our results depend on the changing understanding of string networks. The "BB-AS" (Bennett and Bouchet [16] and Allen and Shellard [17]) parameters are $k_c = 2\pi/\eta$ and $\xi(\eta) = \eta$. The BB-AS simulations tend to show large values ξ/R_H We have intentionally exaggerated their results in this direction by choosing $\xi = \eta$ ($= H \equiv$ "the horizon size"), in order to test the robustness of our conclusions. (For additional information on the string simulations see the contributions on that subject in [18].)

We stress that ξ represent the large scale geometrical features of the network so the *renormalized* μ appears in 6, incorporating the smaller scale features of the string. This renormalization must represent the contributions of the small scale features to the effective linear source denstiy, as discussed in [19].

We plot $(4\pi)(\lambda/(2\pi))^{-3}P(\lambda)$ in Figure 1 (AT = short-dashed, BB-AS = solid, ATO = long-dashed), along with the same curve for perturbations from inflation in CDM [20] (dot-dashed). (We have used for the hubble constant today: $H_0 \equiv 1/R_H = 100h\ km\ sec^{-1}\ Mpc^{-1}$) All the curves have the standard normalization (meant to reproduce the observed galaxy-galaxy correlation function) where the rms $\delta m/m$ in an $R = 8Mpc$ sphere is unity (see Eq 8). This means that μ is different for each curve (see the table below). The slope of all the curves is λ^{-4} for large λ, because the scaling properties of the strings induce the same behavior in $P(\lambda)$ as is produced by the scaling properties of the inflationary perturbations. The transition between radiation and matter domination exposes the differences between strings and inflation. Smaller wavelengths, which enter the horizon in the radiation era have much more power in the string spectrum, compared with inflation spectrum.

Stebbins *et. al.* [21] have shown that wakes produced around the time of equal density in matter and radiation (t_{eq}) have the largest surface density. This fact has been widely interpreted to mean that the dominant long string contributions to the perturbations on many scales come at around t_{eq}. We

have checked this directly by starting the time integration at t_{eq}. The result is much less power on small scales. For example, the BB-AS power is about a factor of ten smaller at $\lambda = 1Mpc$ when the integration starts at t_{eq}. The dominant contributions to small scales are produced before t_{eq}.

We fit the curves in Fig 1 to the form

$$4\pi k^3 P(k) = \frac{\alpha_1 \mu_r^2 4\pi k^4}{1 + (\alpha_2 k) + (\alpha_3 k)^2 + (\alpha_4 k)^3} \left(\frac{1}{1 + (\alpha_5 k)^2} \right)^2 . \qquad (7)$$

The last factor (involving α_5) represents a deviation from λ^{-4} behavior at very large wavelengths. This deviation occurs because the very largest scales have just entered the horizon and have yet to receive their full compliment of perturbations. In Table 1 we present values of the α's which provide a fit to within 10% of the calculated curves: The values of μ_r, which enters

	α_1	α_2	α_3	α_4	α_5	μ_r
AT	45.0	2.30	1.80	0.520	.00127	0.178×10^{-6}
BB-AS	21.8	7.57	5.89	1.93	.000357	0.661×10^{-6}
ATO	37.0	8.95	4.80	1.25	.00112	0.360×10^{-6}

Table 1: Fit parameters (α's) for Eq 7 when k is in units of Mpc^{-1}.The values of μ_r are fixed by the normalization of $P(k)$.

as a parameter in Eq 6, are determined by standard $8Mpc$ normalization condition. The subscript "r" emphasizes that this is the renormalized μ, which incorporates possible effects of the small scale wiggles.

We turn now to a more detailed analysis of our results. The integration over conformal time in Eq 4 covers the entire history of a given scale. At early enough times, any given scale is far outside the Hubble radius and is unperturbed. Around the time when R_H (which always grows faster than $a(t)$) catches up with the comoving scale λ, the string perturbations become uncompensated and $P(\lambda)$ starts to receive significant contributions. The power continues to receive contributions at all later times, but perturbations produced later have less time to grow, and this can diminish their relative contribution to $P(\lambda)$

It will be useful to define the average of any quantity X, by inserting a factor X in the integrand of Eq 4 and then dividing the result by $P(\lambda)$. We write the resulting average $\langle X \rangle_\lambda$. In Fig 2 we plot the average redshift, $\langle z/z_{eq} \rangle_\lambda$, versus wavelength. One can see that different scales get their main contributions at different times. No one time (such as z_{eq}) is singled out.

Although the perturbation theory is performed in Fourier space, the string network is best thought of in position space. The link can be made by the standard formula for mean squared mass perturbation, $\delta m^2/m^2$, inside a sphere of radius R:

$$\left.\frac{\delta m^2}{m^2}\right|_R = \int w^2(x) P(k) 4\pi k^2 dk \tag{8}$$

where $x \equiv Rh^{-1}k$, and $w(x)$, the "window function" is given by:

$$w(x) = \frac{3(\sin(x) - x\cos(x))}{x^3}. \tag{9}$$

We thus define the position space average of any quantity X, by inserting a factor of X in the integrand of 8 and dividing by $\delta m^2/m^2$. The result is labeled $\langle X \rangle_R$.

Figure 3 shows $\langle N_\xi \rangle_R$ where N_ξ is the "number of ξ-times ",

$$N_\xi \equiv \frac{\sqrt{\langle \eta^2 \rangle_\lambda - \langle \eta \rangle_\lambda^2}}{\langle \xi \rangle_\lambda}. \tag{10}$$

The string motions are coherent on a timescale $\Delta\eta \approx \xi$, so Fig 3 shows that most scales are perturbed significantly over more than one string coherence time (although for the BB-AS strings N_ξ is $O(1)$). The relative magnitudes of the three different curves corresponds to the different relative sizes of ξ. The characteristic time over which a given scale is perturbed is similar in the three cases. (The slower coherent string velocities reported in [18] for the AS simulations may suggest a longer coherence time. However, for their large values of ξ, scaling actually requires that a segment of length ξ loose a large fraction its length to loops in just one ξ-time . We feel that the presence of such a disruption on the timescale ξ indicates that ξ is a good measure of the coherence time even for the BB-AS strings.)

If $\lambda > \xi$, the scale λ is being perturbed by many separate string motions occurring on the smaller scale ξ. A box of size λ contains $(\lambda/\xi)^3$ boxes of size

ξ, so one can estimate the number of separate string motions (or "*coherent* string wakes") which contribute to a given scale as $N_c \equiv N_\xi \langle (\lambda/\xi)^3 \rangle_\lambda$, and we plot $\langle N_c \rangle_R$ in Fig 4. One can see that many different wakes contribute to the perturbation on a given scale.

If a string produces a perturbation at a given redshift, z, in the matter era, that perturbation has grown by a factor of z by today. Thus the earliest possible perturbations incur the largest growth. One reason we get large values of N_c is that the perturbations for $\lambda > \xi$ are produced earlier, and thus contribute more to the total perturbation. (Even though $N_\xi = O(1)$ for the BB-AS strings, the contributions come mainly when $\lambda > \xi$, resulting in large values of N_c.) In contrast, perturbations produced in the radiation era do not grow much until the onset of matter domination, so the "growth factor" flattens out. The fact that strings significantly perturb the surrounding matter on scales smaller than the horizon combined with the flatter growth factor causes the dominant contributions to come for $\lambda < \xi$ on scales which entered the horizon far enough back in the radiation era. This is the reason why N_c gets smaller for small R. It is also the reason why the string spectrum has more power on small scales than the inflation spectrum. If the perturbations on a given comoving scale are dominated by the effects of the strings just when that scale crosses the horizon, then a spectrum similar to the inflation spectrum results [5]. The fact that in the radiation era the strings add significant contributions well after the horizon crossing boosts the power on small scales relative to inflation.

As originally pointed out by Vachaspati [22], it is tempting to think that individual string wakes could be responsible for the sheet-like structures in the distribution of galaxies observed on scales of around $50h^{-1}Mpc$ [23]. For this effect to arise, one needs a single coherent string motion to produce the dominant perturbation on a *range* of scales, so that the single wake dominates inside many spheres of different radii which contain the wake. Figure 2 is not encouraging in this regard, since it tells us that the average contribution to the perturbation on each scale comes at different times.

If one centers a sphere of radius R on a planar string wake then, using [21], the perturbation today (in linear theory) is given by $\delta m/m = \frac{3}{2}\Delta R^{-1}$, where Δ is the distance out to which matter has been accreted. (Δ depends on the time when the wake was produced, and is proportional to $\mu_r s$.) For a wake to produce a distinctive effect, $\delta m/m$ around the wake must stand out above the rms $\delta m/m$ on a range of scales. The straight lines in Figure 5

show the $\delta m/m$ around individual wakes. The curves show the rms $\delta m/m$. For each set of string parameters, we calculate two string wake lines. One corresponds to when $\xi = 50Mpc$ and the other is chosen so that Δ takes on its maximum value ($\Delta = 1.5 \times 10^6 \mu_r h^{-2} Mpc$), which occurs at about $z = 2z_{eq}$ (see [21]) and corresponds to different ξ's for different string parameters. When R is about half the mean separation of wakes ($\approx \xi/2$), the value of $\delta m/m$ around the wake should be no different than the contribution to the rms value of $\delta m/m$ produced by those wakes. We terminate the single-wake lines at $R = \xi/2$. Depending on what fraction of the rms $\delta m/m$ a particular wake contributes, the endpoint of the corresponding line may lie close to or below the rms $\delta m/m$ curve. (The three $\xi = 50Mpc$ lines may be identified because they all terminate at $R = 25Mpc$.) We should note that since the single wake lines do not include the effects of compensation, they are actually upper bounds.

Figure 5 shows that even though the perturbation around a given wake increases with decreasing R, the rms $\delta m/m$ is increasing at a similar rate. Since the *slope* of the rms $\delta m/m$ is close to that of the single wake $\delta m/m$, the individual wake does not stand out except on scales orders of magnitude smaller than $50h^{-1}Mpc$. On the larger scales, it gets strong competition from the total $\delta m/m$, which includes contributions from different wakes at different times. (It is possible that when loops are properly accounted for the single wake lines will not rise above the rms $\delta m/m$ on *any* scale, but if they do, that fact could be relevant to galaxy formation.) To the extent that many uncorrelated string motions contribute to the perturbation spectrum, the perturbations are more "gaussian" than previously suspected. We discuss this issue further in [11].

In conclusion, our picture of perturbations from cosmic strings in CDM has been significantly changed by a more systematic analysis. We have shown that the perturbation spectrum is the result of many uncorrelated string motions occurring at different times. The resulting spectrum has much more power on small scales, as compared with inflation, and also as compared with earlier pictures of perturbations from strings. The contributions of many string motions make it unlikely that distinctive "stringy" features will show up strongly in the matter distribution today. Our conclusions assume a scaling string network, but otherwise depend very little on the string network parameters.

Although the relationship between the linear perturbation spectrum

and the astrophysical observations is not well understood, we note that, based on current thinking, the string spectrum does not look good in this regard. The extra power in the string spectrum on small scales feeds into the normalization (that is, it contributes to the galaxy-galaxy correlation function). As a result the amplitude on large scales is reduced, as compared with inflation (see Fig 1). To the extent that the inflationary CDM spectrum is in trouble for lack of power on large scales (as argued, for example, in [24]), one would expect the string induced CDM spectrum to have even greater problems.

We thank Robert Brandenberger for useful conversations. This work was supported in part by the DOE and the NASA (grant NAGW-1340) at Fermilab.

References

[1] T.W.B. Kibble. *J. Phys. A*, 9, 1976.

[2] Ya. B. Zel'dovich. *Mon. Not. Roy. Astron. Soc.*, 192:663, 1980.

[3] A. Vilenkin. *Phys. Rev. Lett.*, 46:1169, 1981.

[4] N. Turok. *Phys. Lett.*, 126B, 1983.

[5] A. Vilenkin and Q. Shafi. *Phys. Rev. Lett.*, 51, 1983.

[6] N. Turok. *Nucl. Phys.*, B242:520, 1984.

[7] J. Silk and A. Vilenkin. *Phys. Rev. Lett.*, 53, 1984.

[8] N. Turok. *Phys. Rev. Lett.*, 55:1801, 1985.

[9] R. Brandenberger and N. Turok. *Phys. Rev. D*, 33:2182, 1986.

[10] S. Veeraraghavan and A. Stebbins. *Ap. J.*, 365, 1990.

[11] A. Albrecht and A. Stebbins. In preperation, 1991.

[12] E. J. Copeland, T. W. B. Kibble, and Daren Austin. Scaling solutions in cosmic string networks. Imperial preprint IMPERIAL/TP/90-91/19, 1991.

[13] A. Stebbins. In G. Gibbons, S. Hawking, and T. Vachaspati, editors, *The formation and evolution of cosmic strings*. Cambridge University Press, 1990.

[14] A. Albrecht and N. Turok. *Phys. Rev. D*, 40:973, 1989.

[15] A. Albrecht and N. Turok. Evolution of cosmic strings. *Phys. Rev. Lett.*, 54:1868, 1985.

[16] D. Bennett and F. Bouchet. *Phys. Rev. D*, 41:2408, 1990.

[17] B. Allen and P. Shellard. *Phys. Rev. Lett.*, 64:119, 1990.

[18] G. Gibbons, S. Hawking, and T. Vachaspati, editors. *The formation and evolution of cosmic strings*. Cambridge University Press, 1990.

[19] T. Vachaspati and A. Vilenkin. Large-scale structure from wiggly cosmic strings. TUP-91-5, 1991.

[20] J. Bardeen *et. al. Ap. J.*, 304, 1986.

[21] A. Stebbins *et. al. Ap. J.*, 322, 1987.

[22] T. Vachaspati. *Phys. Rev. Lett.*, 57, 1986.

[23] M. Geller and J. Huchra. *Nature*, 246, 1989.

[24] W. Saunders *et. al. Nature*, 349, 1991.

Figure Captions

Figure 1: The logarithm of $4\pi(\lambda/2\pi)^{-3}P(\lambda)$ vs. $\log(\lambda)$ for inflation (dot-dashed), AT strings (short-dashed), BB-AS strings (solid) and ATO strings (long-dashed). We use $h = \Omega_0 = 1$

Figure 2: The the average redshift at which each scale is perturbed ($\langle z/z_{eq}\rangle_\lambda$) vs. λ for AT strings (short-dashed), BB-AS strings (solid) and ATO strings (long-dotted).

Figure 3: The number of string coherence times ($\langle N_\xi\rangle_R$) vs. R for AT strings (short-dashed), BB-AS strings (solid) and ATO strings (long-dashed).

Figure 4: The number of contributing coherent string motions ($\langle N_c\rangle_R$) vs. R for AT strings (short-dashed), BB-AS strings (solid) and ATO strings (long-dashed).

Figure 5: The value of $\delta m/m$ in a ball of radius R, vs. R for AT strings (short-dashed), BB-AS strings (solid) and ATO strings (long-dashed). The curves give the rms $\delta m/m$, and the straight lines give $\delta m/m$ in a ball centered on a single wake.We use $h = \Omega_0 = 1$

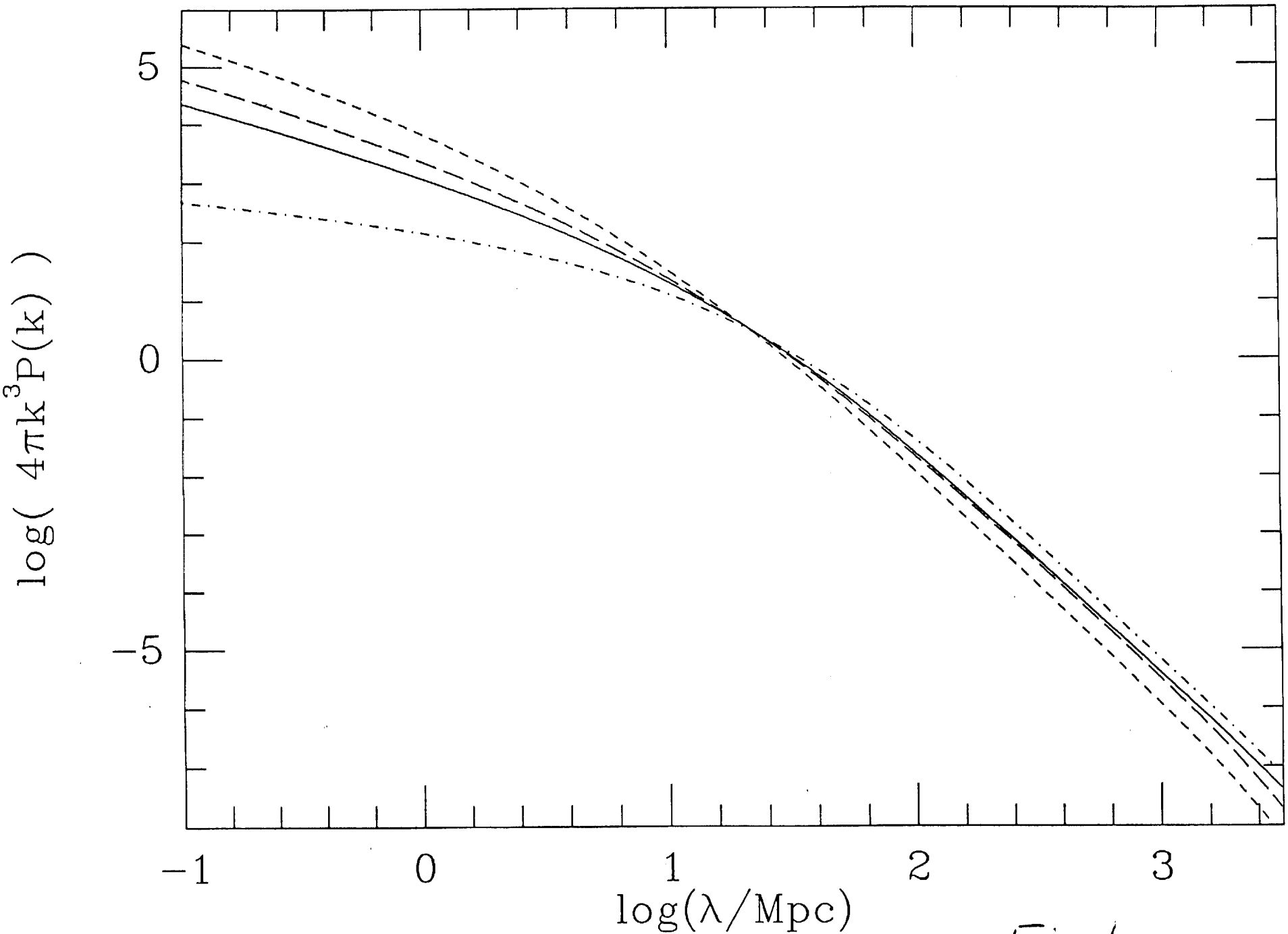

Fig 1

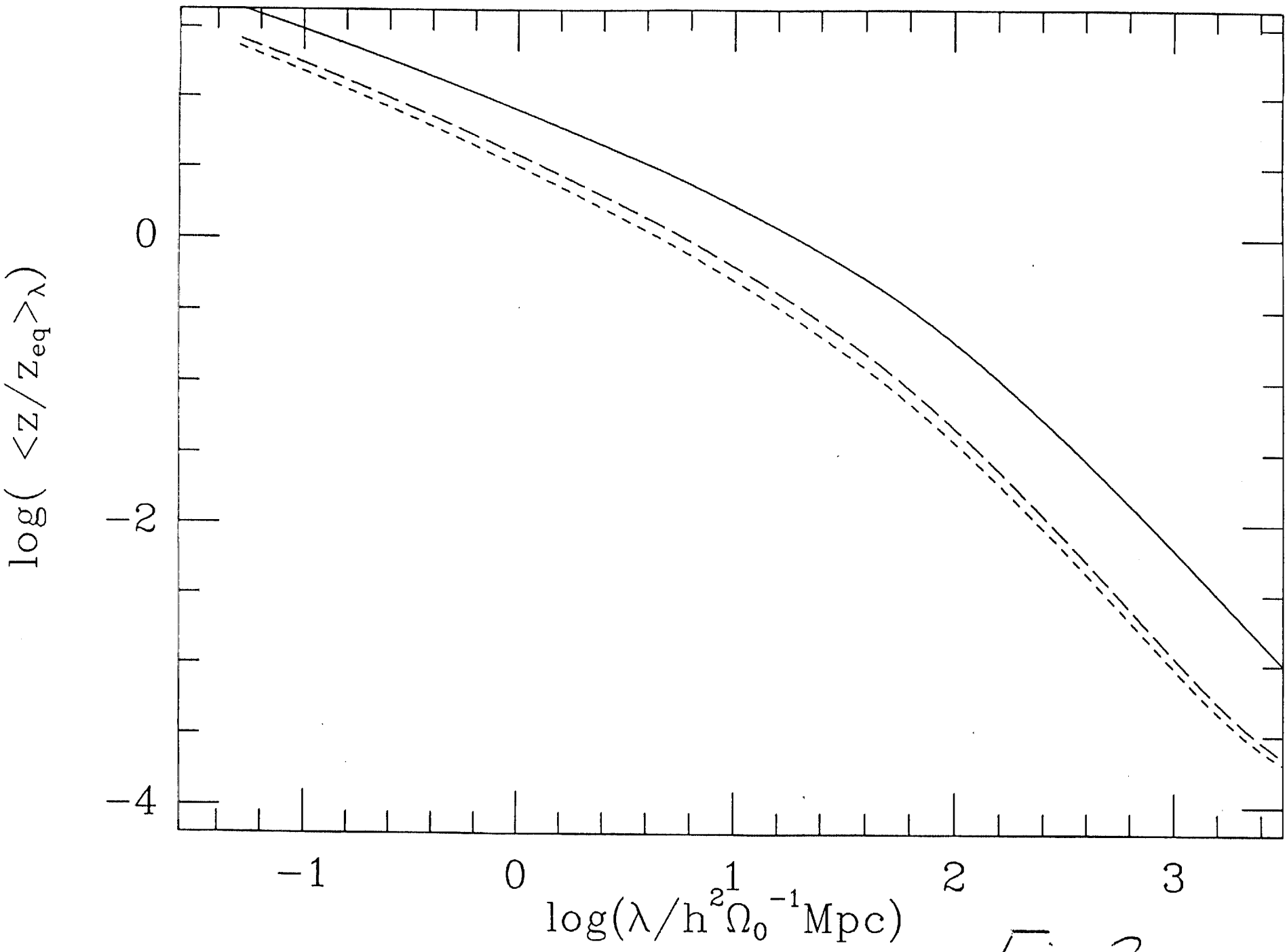

Fig 2

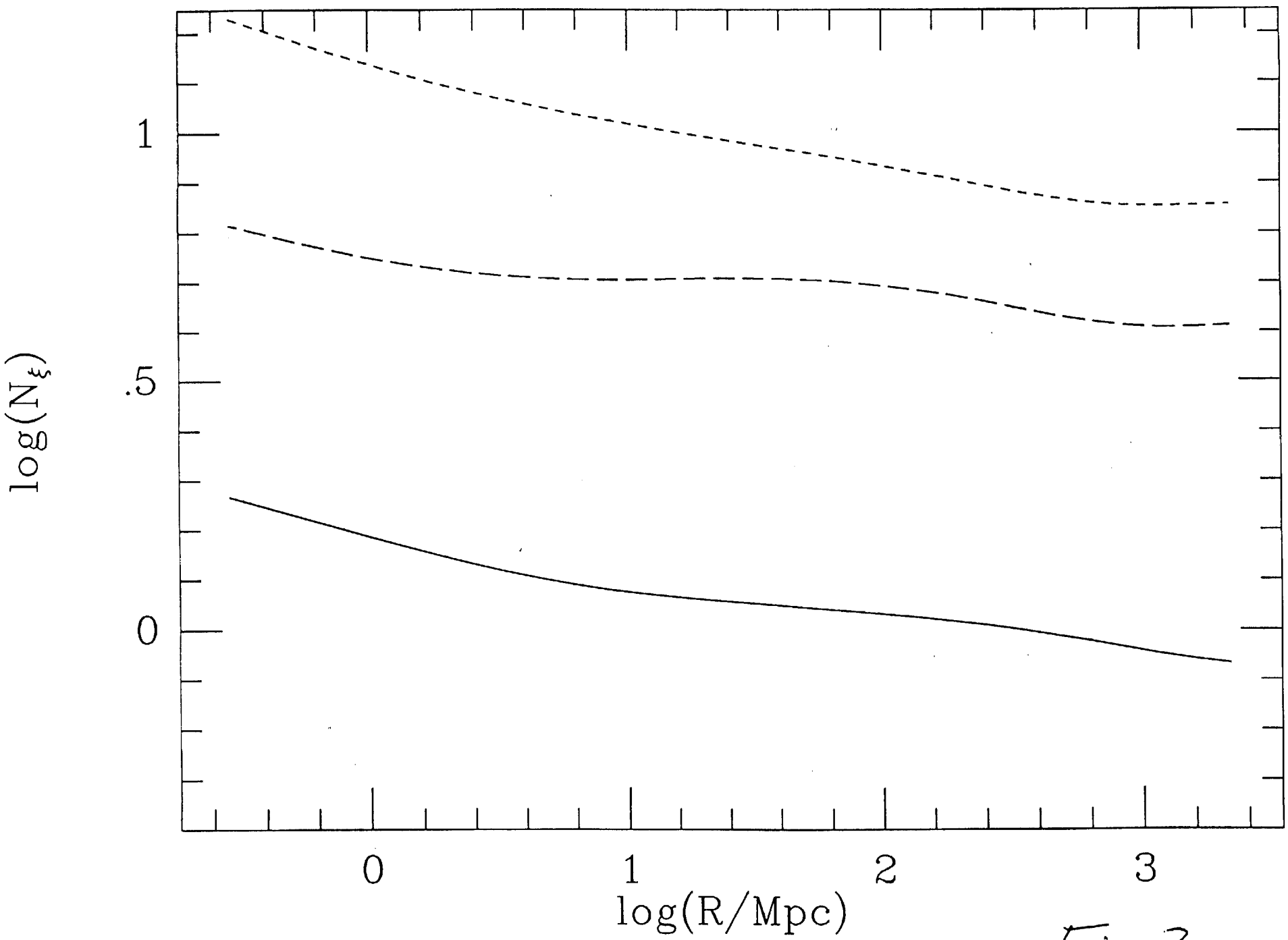

Fig 3

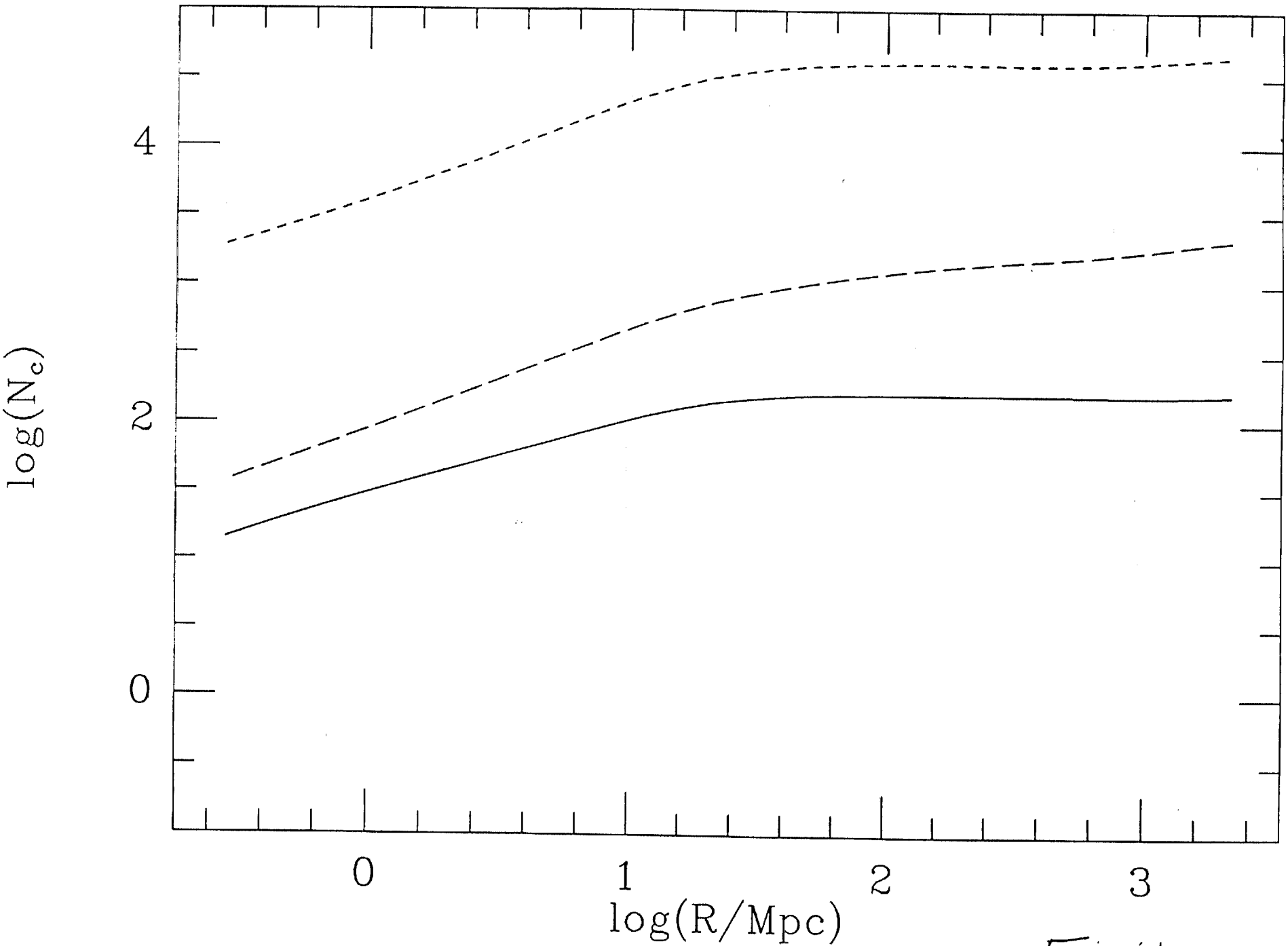

Fig 4

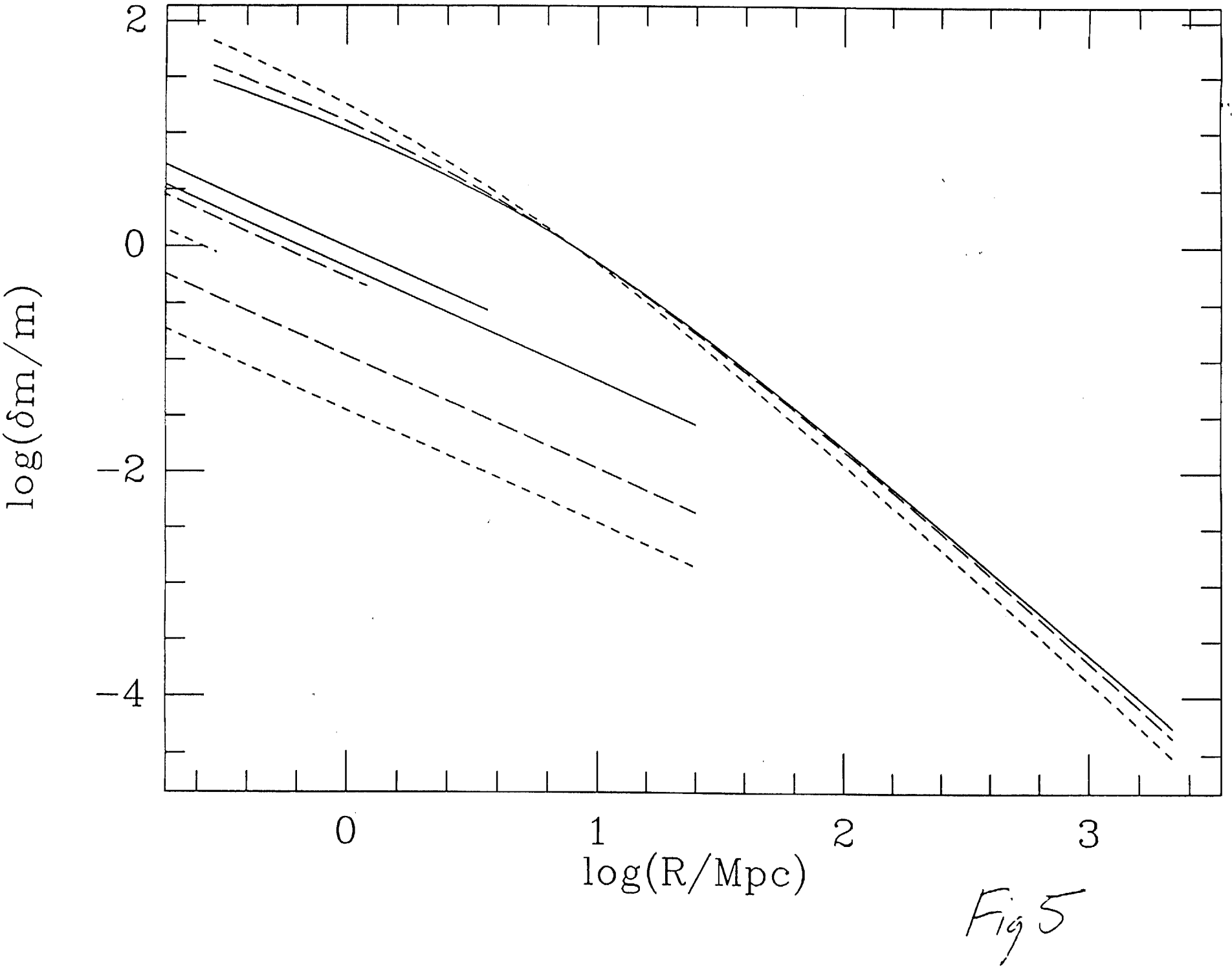

Fig 5